Rare Metal Materials and Engineering
Volume 49, Issue 4, April 2020
Available online at www.rmme.ac.cn

Science Press

Cite this article as: Rare Metal Materials and Engineering, 2020, 49(4): 1159-1165.

ARTICLE

Strengthening Mechanism of Two-Stage Double-Peak Aging in 7050 Aluminum Alloy

Ren Jianping[1], Song Renguo[2,3]

[1] Institute of Intelligent Manufacturing Equipment, Taizhou Vocational College of Science and Technology, Taizhou 318020, China; [2] School of Materials Science and Engineering, Changzhou University, Changzhou 213164, China; [3] Jiangsu Key Laboratory of Materials Surface Science and Technology, Changzhou University, Changzhou 213164, China

Abstract: The effects of microstructure evolution on the strength and hardness of 7050 aluminum alloy during a two-stage aging process were examined. The results indicate that a double-peak phenomenon occurs in the double-stage aging of the 7050 aluminum alloy. The hardness and strength of the second aging peak slightly exceed those of the first peak. Transmission electron microscopy observations indicate that the increase in the hardness and strength for the second aging peak is caused by an increase in the amount of the η' phase. Additionally, the synergistic effect of the η' phase and GP zones surpasses the effect of the GP zones alone.

Key words: 7050 aluminum alloy; two-stage double-peak aging; strengthening; microstructure

7050 aluminum alloy is an Al-Zn-Mg-Cu alloy, and exhibits low density, high strength, and good processing performance. It is widely used in the aerospace industry and civil transportation[1-5]. In the 1980s, Yan et al reported a double-peak aging phenomenon during the long-term aging of 7475 aluminum alloy[6]. Song et al observed a similar phenomenon and confirmed that the hardness and stress corrosion resistance (SCR) of the second aging peak exceeded those of the first aging peak[7,8]. Li et al optimized a composite solid solution, investigated special peak aging for 7012, 7509, and 7208 aluminum alloys, and obtained a double-peak effect. However, they did not analyze the resilience[9]. Chen et al examined the universality of double-peak aging in 7000 series aluminum alloys[10]. Strengthening of the first aging peak depends on the GP zone. On the other hand, the strengthening of the second aging peak is classified into two cases based on the difference in the Zn/Mg ratio in the alloy: the strengthening phase of the alloy is mainly η' ($MgZn_2$) when Zn/Mg>2.2, and mainly T′ ($A1_2Mg_3Zn_3$) when Zn/Mg≤2.2. A new approach was proposed to improve the SCR of the alloy without losing strength. However, the strengthening mechanism of double-peak aging was not considered. Deng et al[11] reported that during the subsequent solution treatment, appropriate nano/submicron-scale $MgZn_2$ particles that precipitated during thermomechanical processing inhibited the migration of the grain/sub-grain boundaries and did not induce particle-stimulated nucleation. Hence, the particles caused a significant decrease in the recrystallized fraction. Suitable thermomechanical processing yielded an ultimate tensile strength of 528 MPa and yield strength of 459 MPa, in addition to satisfactory intergranular corrosion resistance. The double-peak phenomenon of the increase in strength and hardness after ultra-long aging is termed as “double-peak aging”. However, a low-temperature and long double-peak aging process are not suitable for modern industrial production[12,13]. Therefore, the effects of microstructure evolution on alloy strength and hardness during the two-stage double-peak aging of 7050 aluminum alloy were examined in the present study. The two-stage process provided a theoretical foundation to determine a heat-treatment technology that is more suitable for industrial production.

1 Experiment

The 7050 aluminum alloy sheet (produced by ALCOA

Received date: April 25, 2019
Foundation item: National Natural Science Foundation of China (50771093, 51371039)
Corresponding author: Song Renguo, Ph. D., Professor, School of Materials Science and Engineering, Changzhou University, Changzhou 213164, P. R. China, Tel: 0086-519-86330069, E-mail: songrg@hotmail.com

Company, USA) had a thickness of 55 mm, and the heat-treatment sample size was 15 mm×15 mm×10 mm. Its chemical composition (mass fraction, %) was 6.42 Zn, 2.25 Mg, 2.02 Cu, 0.13 Zr, 0.03 Ti, 0.10 Mn, 0.04 Cr, 0.11 Fe, 0.07 Si, and the balance was Al.

Solution treatment was performed in an air furnace at a solution temperature of 743±5 K for a solution treatment time of 70 min. After quenching with water, aging treatment was performed in an electric blast drying oven, for which the temperature precision was controlled to ±5 K. The heat treatment parameters are summarized in Table 1.

A hardness test was performed using an HR-150 Rockwell hardness tester to measure the average hardness of the five points. Prior to the test, the surface of each sample was polished using 200#, 400#, 600#, 800#, 1000#, and 1200# sandpapers to remove the oxide film formed during the heat treatment. Subsequently, the samples were washed with alcohol and dried. The tensile specimens were sampled along the L-T (L-length/longitudinal; T-width/long transverse) direction based on the GB/T16865-1997 standard. Subsequently, they were tested on a Shimadzu AG-10TA universal testing machine, and three samples were measured and averaged. All tension tests were performed at a strain rate of 1×10^{-5} s^{-1} at room temperature. Prior to the hardness and tension tests, all the samples were heat treated in accordance with Table 1.

The samples were ground, polished, and subjected to corrosion testing by applying standard Keller's reagent (2.5% HNO_3+1.5% HCI+1.0% HF+95% H_2O, volume fraction). Transmission electron microscopy (TEM) and scanning electron microscopy (SEM) were employed to analyze the microstructure and fracture morphology. The composition was analyzed using an energy dispersive X-ray spectrometer (EDS) on the scanning electron microscope.

2 Results and Discussion

2.1 Mechanical properties

Fig.1 shows the mechanical properties, namely, the hardness, strength and elongation of the 7050 aluminum alloy during two-stage aging. The results indicate that an M-type double-peak phenomenon occurs. The trends of hardness and strength are essentially consistent, indicating that a double-peak phenomenon occurs during the two-stage aging in 7050 aluminum alloy. Additionally, the hardness and strength for the second peak slightly exceed those of the first peak. The elongation decreases with aging, although it exhibits a slight increase at each peak position. The strength and hardness decrease with the increase in the second-stage aging temperature. A comparison of Fig.1a with 1c indicates that the alloy exhibits higher strength and hardness at the first-stage aging temperature of 393 K. Therefore, maximum hardness and strength as well as good elongation are obtained via long-term aging under the conditions of 743 K/70 min+393 K/ 8 h+423 K/ various aging time. The mechanical properties of the first peak are as follows: the hardness is 92.3 HRB; the ultimate tensile strength (UTS) is 580 MPa; and the elongation is 13.4%. For the valley: the hardness is 82.4 HRB; the UTS is 552 MPa; and the elongation is 13.0%. Finally, for the second peak: the hardness is 93.1 HRB; the UTS is 589 MPa; and the elongation is 12.8%. It should be noted that the second peak aging time during the two-stage double-peak aging is evidently shorter than that during single-stage double-peak aging, as reported previously[7,8].

Table 1 Heat treatment parameters for the 7050 aluminum alloy

Sample	Heat treatment parameters
A	743 K/70 min+383 K/8 h+423 K/varying aging time
B	743 K/70 min+383 K/8 h+433 K/varying aging time
C	743 K/70 min+393 K/8 h+423 K/varying aging time
D	743 K/70 min+393 K/8 h+433 K/varying aging time

2.2 Microstructure

2.2.1 Microstructure at the first peak

Fig.2a and 2b show the intragranular structure and grain boundary structure of the 7050 aluminum alloy for the first aging peak under the condition of 743 K/70 min+393 K/8 h+423 K/17 h. Fig.3a shows that the coherent GP zones are fine and dispersed with a spherical structure. The GP zones are mainly formed and uniformly distributed in the crystal[14].

Small GP zones can be easily cut by dislocations, and various favorable phases produce coplanar slips that form a slip zone[15]. This leads to the accumulation of dislocations near the grain boundary, thereby inducing a local stress concentration and reducing the plasticity of the alloy. Thus, the alloy with the main strengthening phase of the GP zones in the matrix precipitates (MPt) exhibits a relatively low strength. When the matrix deforms, various favorable positions concurrently slip through the dislocations movement with several slip systems; this is followed by further slipping. The transfer continues and reduces the effective cross-sectional area of the GP zones on the slip surface, and even leads to the dissolution of the GP zones. At this stage, a severely deformed slip band is generated and stress concentration occurs near the grain boundaries. This decreases the SCR, fracture properties, and plasticity.

2.2.2 Microstructure at the valley

Fig.2c and 2d show the intragranular structure and grain boundary structure of the 7050 aluminum alloy at the lowest hardness and strength under the condition of 743 K/70 min+393 K/8 h+423 K/33 h. As shown in Fig.2c, the GP zones precipitated in the crystal begin to grow and coarsen. The original fine spherical structure transforms into a coarse spherical structure and is elongated. Furthermore, the distance between the GP zones increases, while the density of the GP zones decreases. At the grain boundary, an extremely small

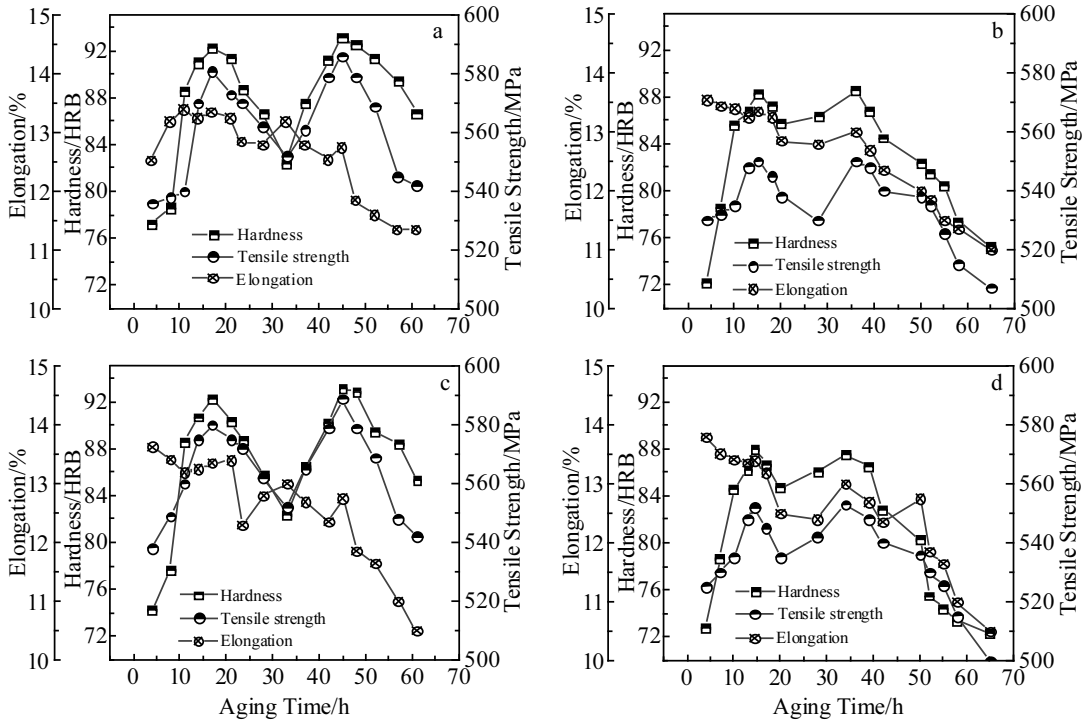

Fig.1 Hardness, strength, and elongation of the 7050 aluminum alloy relative to aging time under various heat treatment: (a) 743 K/70 min+383 K/8 h+423 K/various aging time, (b) 743 K/70 min+383 K/8 h+433 K/various aging time, (c) 743 K/70 min+393 K/8 h+423 K/various aging time, and (d) 743 K/70 min+393 K/8 h+433 K/various aging time

amount of the η' phases are precipitated. The η' phase particles are extremely small and continuously distributed along the grain boundary. When the aging time increases, the formed GP zones begin to coarsen. Thus, the volume fraction of the GP zones begins to decrease. However, the newly formed η' phase does not hinder the dislocations. Therefore, the hardness begins to decrease sharply. The fact that the elongation is lower than that at the first peak is attributed to the increase in the uneven deformation within the crystal and the decrease in the grain boundary strength.

2.2.3 Microstructure at the second peak

Fig.2e and 2f show the intragranular structure and grain boundary structure of the 7050 aluminum alloy at the highest hardness and strength under the condition of 743 K/70 min+393 K/8 h+423 K/45 h. As shown in Fig.2e, only a part of the GP zones remains in the large circular region. The η' phases precipitate in the crystal and are uniformly distributed, which are needle-like and extremely small although their volume fraction is high, as shown in Fig.3b. The η' phase on the grain boundary begins to aggregate and coarsen and subsequently begins to transform into a smooth η phase that is discontinuously distributed on the grain boundary, as shown in Fig.2f. This phenomenon is consistent with the reports by Song et al[7]. A few η' phases begin to aggregate on the grain boundary. They become coarse and gradually transform into an incoherent η phase, thereby gradually decreasing the energy of the system. The structure is advantageous in terms of the development of matrix deformation.

After the alloy enters the bottom of the valley, the GP zones in the crystal grow and gradually disappear as aging progresses. During the aging process, multiple small GP zones exist and overcome the high barriers of strontium formation. This is favorable for the η' phase nucleation. Additionally, several high-energy distortion fields are formed in the coarse GP zones at the bottom of the valley, which offers energy conditions for the formation of the η' phase. At this stage, the activation energy of the precipitate phase is considered as the formation activation energy of the η' phase. A large amount of η' phases are formed under the favorable conditions. The η' phase is fine and exhibits a dispersed distribution, and the strength of the alloy gradually increases. When the size, density, and distribution of the η' phase in the alloy reach a certain threshold, the alloy exhibits a second aging peak that exceeds the first aging peak in terms of hardness and strength. The increase in strength and hardness suggests that a large amount of the η' phases are better than the independent enhancement of the GP zones. Consequently, the dislocations cannot be cut through the η' phases; it is only possible to bypass them. The strengthening effect improves, although the total density of the precipitate phases decreases. The η' phases are distributed uniformly in the matrix; consequently, the deformation is uniform. This leads to a significant increase in plasticity.

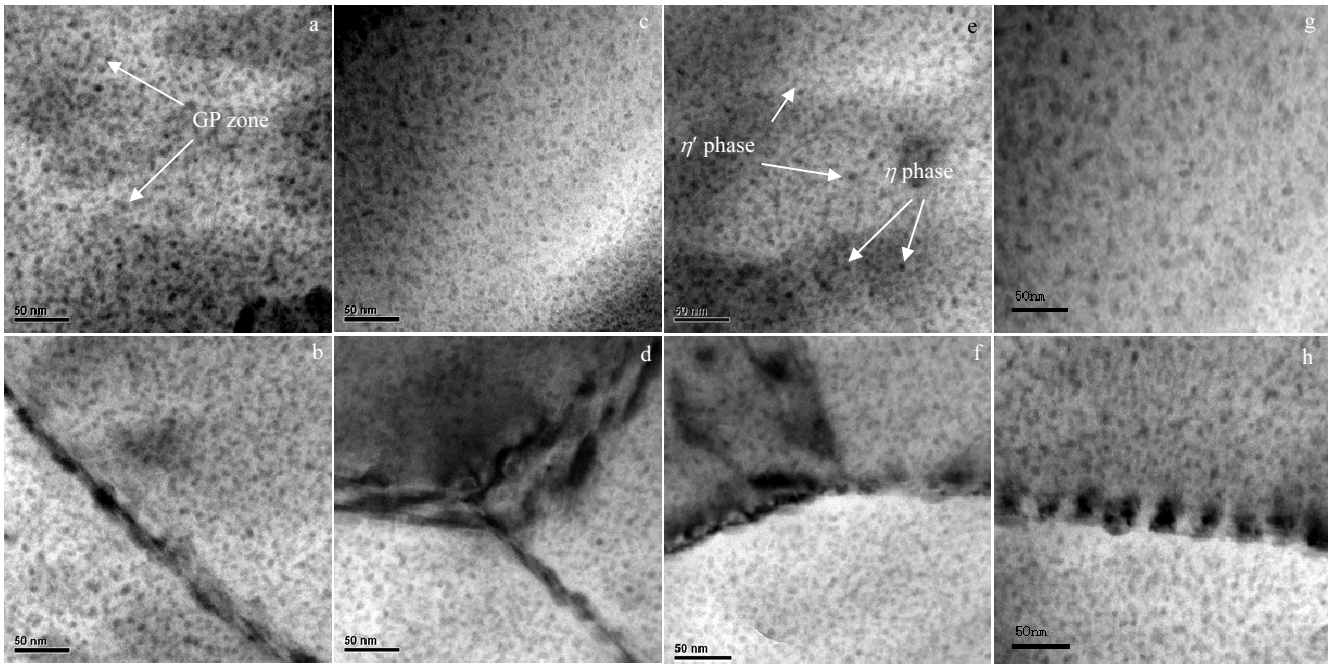

Fig.2 Intragranular (a, c, e, g) and grain boundary (b, d, f, h) structure of the 7050 aluminum alloy: (a, b) 743 K/70 min+393 K/8 h+423 K/17 h, (c, d) 743 K/70 min+393 K/8 h+423 K/33 h, (e, f) 743 K/70 min+393 K/8 h+423 K/45 h, and (g, h) 723 K/70 min+393 K/8 h+423 K/57 h

The MPt is dominated by the η' phase that was obtained via the blocking effect of the second phase on the dislocations, namely the Orowan mechanism. Therefore, an excessive-strength weak zone is not produced[16,17]. The objective of alloy aging treatment from single-stage aging to two-stage aging is to obtain a higher amount of the η' phase and a certain amount of the η phase. If the MPt is considered only from the strength viewpoint, a higher volume fraction yields greater dispersion and a better strengthening effect irrespective of the type of particle that is used as the strengthening phase. The high strength of the precipitated phase and a uniform distribution are apparently advantages for the SCR and toughness because the uniformly distributed high-strength particles more effectively hinder the movement of the dislocations during the deformation, and the stress concentration is low[18].

2.2.4 Microstructure at the overaged state

Fig.2g and 2h show the intragranular structure and grain boundary structure of the 7050 aluminum alloy in the overaged state under the condition of 743 K/70 min+393 K/8 h+423 K/57 h when the hardness and strength begin to decrease. As shown in Fig.2g, the intragranular η' phase grows and transforms into the η phase under equilibrium. The transformed η phase begins to coarsen, and the original fine needle-like phases decrease and eventually disappear. The coarse slab-like structure dots at the beginning of the increase and the discrete phase of the η phase on the grain boundary exhibits larger particles. Subsequently, a large-scale intermittent phenomenon emerges, as shown in Fig.2h. Thus, a continuous

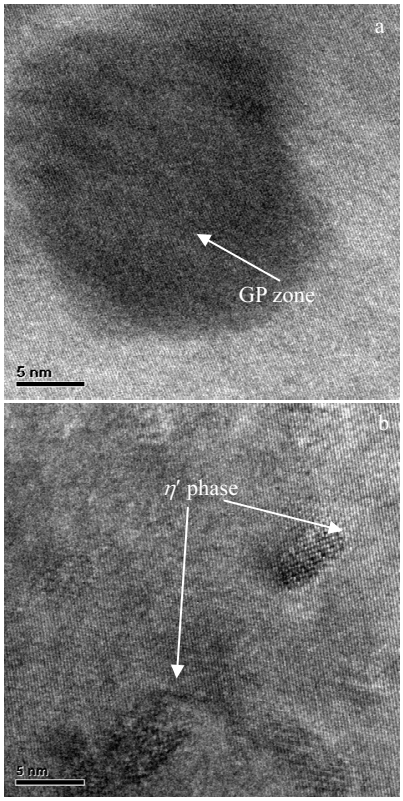

Fig.3 High-resolution intragranular images of the 7050 aluminum alloy: (a) 743 K/70 min+393 K/8 h+423 K/17 h and (b) 743 K/70 min+393 K/8 h+423 K/45 h

network of grain boundary precipitates appears. The precipitation of the continuous network is harmful to the performance and especially to the SCR of the alloy because corrosion microcells easily form on the grain boundary[19,20].

2.3 Strengthening mechanism of two-stage double-peak aging

The strength, hardness, SCR, and fracture toughness of the material can be improved by changing the size, shape, and distribution of the precipitated phase[21,22]. The aging precipitation sequence of the alloy changes from the GP zone to the η' phase. Subsequently, the η' phase gradually coarsens and transforms into the equilibrium η phase. During this period, the hardness and strength values exhibit two peaks with aging in terms of hardness and strength. The second peak slightly exceeds the first peak. From a microstructural viewpoint, the second increase in strength indicates that the combination of the η' phase and GP zones is better than the effect of the GP zones on its own. The enhancement of the first hardness peak occurs because the high-density GP zones consume a high amount of energy when the dislocations cut through the GP zones. The second hardness peak increases to a certain extent when compared to the first hardness peak, and this is because the dislocations are not cut through and only bypass the η' phase. After the first peak, the second-phase size increases (in the second high-temperature period), and the matrix loses coherence. The GP zones decrease, and the density of the precipitated phases decreases. However, the strengthening effect is enhanced. The second peak is shown macroscopically in Fig.4, which indicates a clear relationship between the hardness as well as the dissolution phase structure and aging time of the 7050 aluminum alloy during aging. When the aging time increases, the strength decreases because the precipitated phase of the alloy grows, the spacing increases, and over-aging occurs.

2.4 Fractograph analysis

Fig.5 shows the fracture surface SEM images of the 7050 aluminum alloy under various heat-treatment regimes. The aging system is 743 K/70 min+393 K/8 h+423 K/varying aging time. As shown in Fig.5c, the fracture morphology at the second aging peak of the 7050 aluminum alloy exhibits dimples with almost uniform sizes. The ratio of the dimples evidently exceeds that under other heat-treatment systems. Therefore, the fracture morphology indicates that the plasticity of 743 K/70 min+393 K/8 h+423 K/45 h is optimal. Furthermore, dimples are observed in the fracture morphology shown in Fig.5a. Although

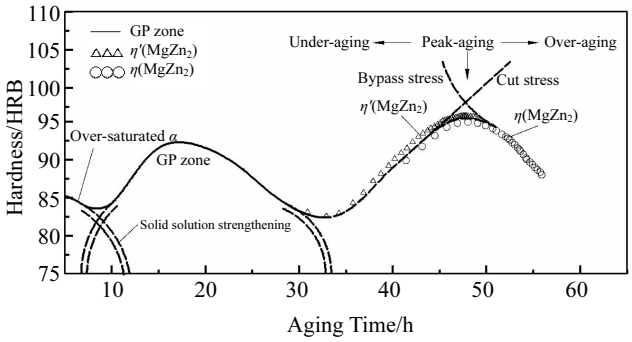

Fig.4 Relationship between the hardness as well as dissolution phase and aging time of the 7050 aluminum alloy

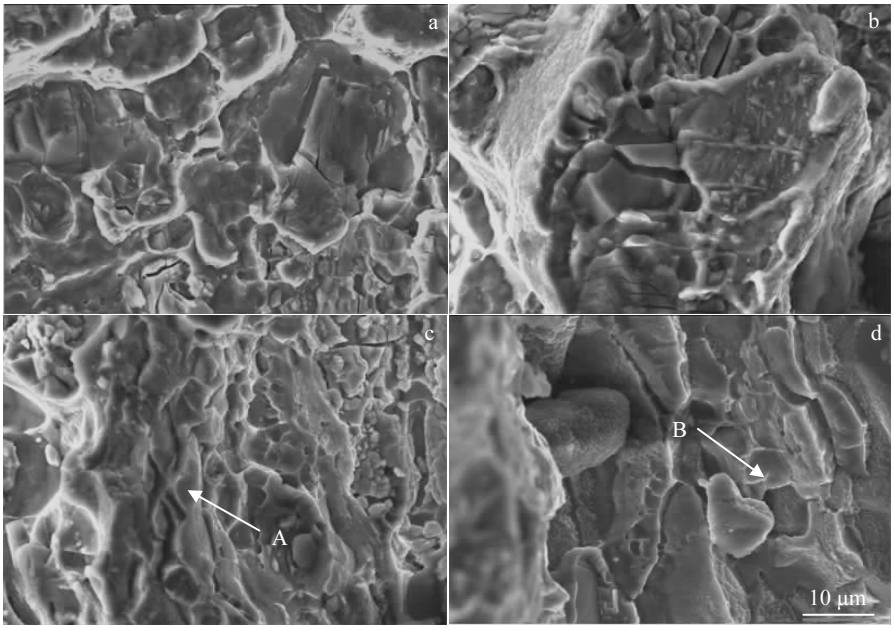

Fig.5 Fracture surface SEM images of the 7050 aluminum alloy under various heat-treatment regimes: (a) 17 h, (b) 33 h, (c) 45 h, and (d) 57 h

Table 2 EDS analysis results of points A and B in Fig.5 (wt%)

Point	Zn	Mg	Cu	Zr	Ti	Mn	Cr	Fe	Si	Al
A	6.42	2.25	2.02	0.13	0.03	0.10	0.04	0.12	0.06	Bal.
B	6.42	2.20	2.05	0.12	0.02	0.10	0.05	0.48	0.39	Bal.

there are few dimples, intergranular fracture is dominant and there are hard and brittle points at the bottom of the dimples. Shearing pieces are also observed, indicating that the microstructure of the state is brittle. As shown in Fig.5b and 5d, there are few dimples, with several hard and brittle phase particles. Pores or voids are generated at the interface between the particles and matrix. Thus, micro-cracks are also generated, and the crack propagation causes the matrix to disconnect from the periphery of the particle to form pit-shaped dimples of various sizes and depths. The EDS analysis was performed on the particles at points A and B, as shown in Fig.5c and 5d. The analysis results are presented in Table 2.

With the exception of Fe and Si, the other elements at points A and B are essentially similar. The contents of Fe and Si at A are significantly lower than those at B, potentially because the contents of Fe and Si significantly affect the plasticity[23-25]. A particle is located at the center of a dimple and is the source of a crack. Under the action of an external force, the dislocation is pushed to the second-phase particle. The hard and brittle particles accumulate. When several dislocation loops are pushed to the interfaces between the particles and the substrate, micropores form separately, and the new dislocation loop is continuously pushed toward the micropores, thereby rapidly expanding them. Finally, the material fails.

3 Conclusions

1) There exists a double-peak phenomenon during the two-stage aging process of 7050 aluminum alloy. The hardness and strength of the second peak slightly exceed those of the first peak. The elongation decreases with the increasing aging time, although it slightly increases at each peak position. Two-stage double-peak aging is more suitable for industrial production.

2) For the first peak, the hardness is 92.3 HRB, the UTS is 580 MPa, and the elongation is 13.4%. For the valley, the hardness is 82.4 HRB, the UTS is 552 MPa, and the elongation is 13.0%. For the second peak, the hardness is 93.1 HRB, the UTS is 589 MPa, and the elongation is 12.8%.

3) The strengthening of the first aging peak is attributed to the high-density GP zones, while that of the second aging peak is attributed to the combination of the η' phase and GP zones.

References

1 Zhang W W, Hu Y, Zhang G Q *et al. Metals*[J], 2017, 7(10): 425

2 Qi X, Song R G, Qi W J *et al. Journal of Wuhan University of Technology-Materials Science Edition*[J], 2017, 32(1): 173

3 Hu H E, Wang X Y. *Metals*[J], 2016, 6(4): 79

4 Qi X, Jin J R, Dai C L *et al. Materials*[J], 2016, 9(11): 884

5 Qi X, Song R G, Qi W J *et al. Rare Metal Materials and Engineering*[J], 2016, 45(8):1943

6 Yan D J. *Journal of Materials Engineering*[J], 1992(2): 15 (in Chinese)

7 Song R G, Dietzel W, Zhang B J *et al. Acta Materialia*[J], 2004, 52(16): 4727

8 Song R G, Geng P, Zeng M K *et al. Journal of Materials Science and Technology*[J], 1998, 14(3): 259

9 Li C M, Chen Z Q, Cheng N P *et al. Light Alloy Fabrication Technology*[J], 2007, 35(12): 36 (in Chinese)

10 Chen X M, Song R G. *Hot Working Technology*[J], 2009, 38(2): 93 (in Chinese)

11 Deng Y L, Zhang Y Y, Wan L *et al. Materials Science and Engineering A*[J], 2012, 554: 33

12 Peng G S, Chen K H, Chen S Y *et al. Materials Science and Engineering A*[J], 2011, 528(12): 4014

13 Milkereit B, Österreich M, Schuster P *et al. Metals*[J], 2018, 8(7): 531

14 Viswanadhan R K, Sun T S, Green J A S. *Metallurgical and Materials Transactions A*[J], 1980, 11: 85

15 Liu J H, Li D, Liu P Y *et al. The Chinese Journal of Nonferrous Metals*[J], 2002, 12: 208 (in Chinese)

16 Gazda A, Warmuzek M, Wierzchowski W. *Thermochimica Acta*[J], 1997, 303(2) : 197

17 Brown B F. *Stress Corrosion Cracking in High Strength Steels and in Titanium and Aluminum Alloys*[M]. Washington: Naval Research Laboratory, 1972

18 Alarm A, Bahr D F, Jacroux M. *Corrosion Science*[J], 2006, 48(4): 925

19 Najjar D, Magnin T, Warner T J. *Materials Science and Engineering A*[J], 1997, 238(2): 293

20 Guseva O, Schmutz P, Suter T *et al. Electrochim Acta*[J], 2009, 54(19): 4514

21 Gest R J, Troiano A R. *Corrosion*[J], 1974, 30(8): 274

22 Oriani R A, Josephic P H. *Acta Metall*[J] 1974, 22(9): 1065

23 Pressouyre G M. *Acta Metall*[J] 1980, 28(7): 895

24 Chu W Y, Qiao L J. *Fracture and Environmental Fracture*[M]. Beijing: Science Press, 2000 (in Chinese)

25 Scamans G M, Holroyd N J H, Tuck C D S. *Corrosion Science*[J], 1987, 27(4): 329

7050 铝合金双级双峰时效强化机理

任建平[1]，宋仁国[2,3]

(1. 台州科技职业学院 智能制造装备研究所，浙江 台州 318020)

(2. 常州大学 材料科学与工程学院，江苏 常州 213164)

(3. 常州大学 材料表面科学与技术重点实验室，江苏 常州 213164)

摘　要：系统地研究了 7050 铝合金双级双峰时效微观组织对强度和硬度的影响。 结果表明，7050 铝合金的双级时效出现了双峰现象，第 2 峰的硬度和强度均略高于第 1 峰。高分辨透镜（HRTEM）观察表明，第 2 峰值的硬度和强度的增加是由于一定数量的η'相数量的增加引起的。此外，η'相和 GP 区的共同作用优于 GP 区单独的效果。

关键词：7050 铝合金；双级双峰时效；机械强度；微观组织

作者简介：任建平，男，1983 年生，硕士，副教授，台州科技职业学院智能制造装备研究所，浙江 台州 318020，电话：0576-89188347，E-mail: renlinbo411@163.com